EVALUATION OF HOT CRACKING SUSCEPTIBILITY OF SOME AUSTENITIC STAINLESS STEELS AND A NICKEL-BASE ALLOY




G. Srinivasan **A.K. Bhaduri[a]** **V. Shankar[b]** **B. Raj**

Indira Gandhi Centre for Atomic Research (IGCAR), (India)
[a] Email: bhaduri@igcar.gov.in; [b] formerly with IGCAR

ABSTRACT

For the Prototype Fast Breeder Reactor (PFBR), a modified version of 316L stainless steel, designated as 316L(N), has been chosen as the major structural material. In order to reduce the risk of sensitisation, the carbon content has been reduced to less than 0.03 wt-%, and to compensate for the loss in strength due to the reduced carbon content the nitrogen content has been specified to be about 0.08 wt-%. For fuel clad and wrapper applications, a radiation-resistant variation of 316 stainless steel containing titanium about 6 times the carbon content, named Alloy D9, has been chosen. Weld metal and heat-affected zone (HAZ) cracking of austenitic stainless steels Alloy D9 and 316L(N) were investigated. Specifically, the role of titanium in Alloy D9 and nitrogen in 316L(N), along with the impurity elements, were studied. In Alloy D9, cracking increased with Ti/C ratio, but a significant contribution to cracking came from the nitrogen of about 200 ppm picked up during welding even when using high purity argon shielding gas. Titanium to carbon (Ti/C) ratio of about 4 was found to show least susceptibility to solidification as well as HAZ cracking. In modified 316 weld metals with 3–7 FN, nitrogen in the range 0.06–0.12 % had no detrimental effect on weldability. Weldability of Inconel 718 base material was also investigated. From hot cracking considerations, ENiCrFe-3 consumable was found more suitable to weld Inconel 718 than consumable of matching composition. Weldability was tested in various geometrical configurations such as T-, butt- and rod-to-strip in similar as well as dissimilar combination with 9Cr-1Mo steel using ENiCrFe-3 consumable. The studies showed the need for careful joint preparation and use of techniques to enhance weld penetration for minimising defects. This paper discusses the weldability problems associated with these austenitic stainless steels chosen for use in the construction of PFBR. Various criteria in use for weldability evaluation as per codes in relation to the present data on stainless steels and nickel-base alloys are also discussed. The importance of hot cracking evaluations in determining the fabrication weldability of these austenitic stainless steels is also discussed in detail.

IIW-Thesaurus keywords: *Austenitic stainless steels; Cracking; Defects; Ductility; Heat affected zone; Hot cracking; Mechanical properties; Reference lists; Solidification cracking; Stainless steels; Steels; Weld metal; Weld zone; Weldability tests.*

1 INTRODUCTION

The nuclear core of a Fast Breeder Reactor (FBR) is geometrically compact and has a high power density. Liquid sodium with its high thermal conductivity and heat capacity is the preferred coolant in FBRs. The elevated operating temperatures (673–973 K) and high fast neutron flux present a very hostile and demanding environment for the materials. The materials chosen must possess adequate strength under the operating conditions. The core structural materials should also be resistant to radiation damage. In general, nuclear grade materials differ from the conventional grades because of the close control of chemical composition,

Doc. IIW-1907-08 (ex-doc. II-1644r1-07/II-C-345r1-07) recommended for publication by Commission II “Arc Welding and Filler Metals”.

lower limits on residual elements and high degree of cleanliness. A variety of austenitic stainless steels is used in fast reactor systems.

Austenitic stainless steels of AISI type 316 (316 SS) and its variants are used extensively as a structural material for the components of FBRs operating at temperature up to 823 K and service life of about 40 years. A major problem encountered during welding of austenitic stainless steels is hot cracking, besides that of sensitisation in the heat-affected zone (HAZ). The problem of sensitisation of the HAZ and the consequent risk of failure by intergranular stress corrosion cracking is minimized by the choice of low carbon varieties of stainless steel. To avoid hot cracking, the composition of the welding consumable is finely adjusted such that the primary mode of solidification remains ferritic [1]. The resultant weld deposit has a duplex microstructure consisting of about 3–10 % delta ferrite in the austenitic matrix [2]. This microstructure is highly unstable and the delta-ferrite on exposure to high temperature undergoes transformation to carbides and a variety of brittle intermetallic phases [3].

A nuclear grade type 316 SS was used as the principal structural material for the Fast Breeder Test Reactor (FBTR) at Kalpakkam, India. For the Indian Prototype Fast Breeder Reactor (PFBR), a modified version of 316L SS, designated as 316L(N) SS, has been chosen as the major structural material. In order to reduce the risk of sensitisation in 316L(N) SS, the carbon content has been reduced to less than 0.03 wt-%, and to compensate for the loss in strength due to the reduced carbon content the nitrogen content has been specified to be about 0.08 wt-%. For fuel clad and wrapper applications, a radiation-resistant variation of 316 SS containing titanium (about 6 times the carbon content), named Alloy D9, has been chosen.

Weldability of two major classes of austenitic materials is of concern with regard to fabrication of the PFBR. These are (i) austenitic stainless steels D9 and 316L(N), and (ii) nickel-base alloy Inconel 718 that are used as material of support structures of the steam generator tubes. In the case of D9 and to a lesser extent for 316L(N), hot cracking in the weld metal and heat-affected zone (HAZ) is a major issue. Weldability concerns of Inconel 718 include hot cracking as well as fluidity and weld bead penetration.

The objectives of the work done on D9 and 316L(N) were to quantify solidification (weld metal) cracking and HAZ cracking as a function of composition using Varestraint hot cracking tests supplemented by detailed microstructural studies. It was also required in the course of the work, to examine criteria relating cracking in the Varestraint test to actual weld behaviour. Hot cracking evaluations in Inconel welds included Varestraint testing to study effect of heat input on cracking in Inconel 718 and Inconel 82. Fabrication weldability studies in different geometrical configurations expected during steam generator fabrication were also carried out. This paper discusses the weldability problems associated with these austenitic materials chosen for use in the construction of PFBR. The importance of hot cracking evaluations, in determining the fabrication weldability of these austenitic materials, is also discussed.

2 DESIGN CONSIDERATIONS FOR HOT CRACKING SUSCEPTIBILITY

Till the late 1980s, design of welded components operating at high temperatures was based solely on the properties of the base metal due to lack of adequate information on the high temperature properties of welds. Nuclear codes now incorporate strength reduction factors based on actual properties of the weld metal [2]. However, these design rules are considered still inadequate since they do not recognise the actual behaviour of weldments.

Various codes for fabrication such as RCC-MR and ASME Section III provide for hot cracking tendency of austenitic stainless steels during welding by either specifying limits on ferrite content in weld metal or by simple usability tests. RCC-MR specifications for welding filler materials make a distinction for ferrite content based on service temperature. As per RS 3334, 5–15 % ferrite is specified for components operating below 648 K (375 °C). For components operating above this temperature, these limits do not apply and the user must specify ferrite limits. Weld ferrite content is determined by either Schaeffler or DeLong diagram or by magnetic saturation method. When ferrite content of the deposited weld is below 5 %, RS 2536 stipulates a groove cracking test for qualification of welding consumables as per RS I 900 or 930. The test, which has also been adopted for PFBR consumables, consists of depositing (undiluted) 5 lengths of weld metal (50 or 60 mm length) within an 80° groove. The deposits are then examined for cracking using liquid penetrant test. Filler materials or electrodes must exhibit freedom from cracking, including crater cracking, to qualify. ASME Section III NB-2433.2 does not make a distinction based on service temperature but accounts for hot cracking tendency by specifying a minimum ferrite level as per WRC-92 ferrite diagram. Similar criteria have been recommended by Lundin *et al*. [4] for nuclear-grade stainless steels including 316L(N). Delta-ferrite is restricted in weld metals intended for elevated temperature service because it results in poor creep properties due to its microstructural instability under service conditions.

As discussed above, the code stipulations rely on conservative tests and additional requirements such as ferrite level specification to provide for resistance to cracking susceptibility. However, the codes do not address adequately tests for hot cracking behaviour of weld metals intended for high temperature service in several areas. The first is the possibility of HAZ cracking in the base metal and multipass stainless steel weld metal that are not taken into account in the codes. The second drawback is that there are no guidelines for weldability evaluation of fully austenitic material

such as D9. There was therefore a need for detailed weldability evaluation of PFBR materials to obtain clear quantitative guidelines for excluding possibility of cracking while at the same time avoiding excessive conservatism.

3 EVALUATION OF HOT CRACKING SUSCEPTIBILITY

Hot cracking is an important problem encountered during the welding of austenitic stainless steels. It is believed that hot cracking occurs by the formation of low-melting phases in the solidifying weld metal and in the HAZ, which causes cracking under the action of shrinkage stresses and restraint imposed on the joint [5]. In the HAZ, cracking occurs by liquation of grain boundaries in the partially melted zone adjacent to the fusion line and in previously deposited weld metal in a multipass weld [6]. Although the problem of hot cracking has been studied for several decades, the mechanism by which many of the impurities and minor elements promote cracking is largely unknown. Further, it was discovered that rather than the residual ferrite content, it is the formation of ferrite as the primary phase during solidification that reduces cracking susceptibility [7]. However, in many applications such as for high temperature or corrosive service, either the weld metal composition may be fully austenitic or ferrite may be restricted to limits that may not permit primary ferrite formation.

Alloy D9, a 15Cr-15Ni-2Mo-0.3Ti fully austenitic stainless steel (roughly corresponding to UNS S38660), has been chosen for core components in the PFBR in view of its resistance to radiation damage [8]. However, the presence of titanium is known to increase cracking in materials like 321 SS [9] and A286 SS [10]. Hence, in Alloy D9, which contains titanium, the relation between composition and cracking was studied to identify the mechanisms of cracking and to optimise the composition in terms of weldability. 316L(N) SS, a nitrogen-bearing modification of 316L SS, has been chosen as the primary structural material for PFBR. Previous studies on the effects of nitrogen in nitrogen bearing austenitic stainless steels have been controversial, some reporting beneficial effects [11] and others neutral or detrimental behaviour [12, 13]. Hence, the role of nitrogen in cracking of 316L(N) weld metal was investigated in detail. Also, in view of the importance of solidification mode, impurities and minor elements in determining cracking behaviour, the correlation between composition and cracking in these austenitic materials was studied. Since a quantitative evaluation of cracking was fundamental to this analysis, the assessment criteria for hot cracking using the Varestraint test was critically examined.

Weldability evaluation of austenitic materials usually involves application of strain or some form of restraint during welding and assessing the deposited weld for cracking [4]. Weldability assessment of austenitic stainless steels and nickel-base alloys was done using the Varestraint test [14]. Evaluation using this test is done using criteria such as total crack length (TCL), maximum crack length (MCL) or brittleness temperature range (BTR). BTR is essentially the temperature range over which weld metal is prone to cracking due to the presence of low melting eutectics during solidification. It is derived from maximum crack length (MCL) by converting length into temperature using the centreline cooling curve and welding speed.

3.1 Materials investigated

Among austenitic stainless steels, three heats of Alloy D9, one heat of 316L(N) SS base metal, one of 316L SS, four of modified 316 weld metal compositions, and a few other materials for reference (Table 1), were eva-

Table 1 – Chemical compositions (in wt-%) of the stainless steel weld metals tested

Material	FN [a]	C [b]	Mn	Cr	Ni	Si	Mo	N [b]	P [b]	S [b]	Other
316L(N)	0.7[(1)]	0.03	1.45	16.8	11.1	0.53	2.06	0.073	0.031	0.001	0.27 Cu
316L	2.6[(2)]	0.029	1.8	17.0	11.9	0.7	2.25	0.036	0.035	0.012	–
D9-A	0	0.052	1.5	15.1	15.0	0.5	2.26	0.066	0.011	0.002	0.21 Ti
D9-B	0	0.051	1.5	15.0	15.1	0.5	2.25	0.068	0.011	0.002	0.32 Ti
D9-C	0	0.052	1.5	15.1	15.3	0.52	2.26	0.064	0.012	0.002	0.42 Ti
316-A	3.9[(2)]	0.049	1.1	18.8	12	0.44	2.5	0.067	0.026	0.012	–
316-B	4.8[(2)]	0.044	1.2	18.4	11.4	0.36	2.5	0.091	0.025	0.015	–
316-C	5.0[(2)]	0.043	1.3	18.7	11.0	0.36	2.5	0.097	0.025	0.016	–
316-D	3.9[(2)]	0.046	1.3	18.4	10.5	0.33	2.5	0.12	0.027	0.015	–
304L-A	0	0.016	1.51	18.12	11.58	0.53	–	0.039	0.023	0.018	–
304L-B	3.0[(2)]	0.023	1.21	19.07	10.46	0.41	–	0.066	0.024	0.012	–
304L-C	2.9[(2)]	0.023	1.67	18.88	10.09	0.42	–	0.069	0.031	0.019	–
321	4.4[(2)]	0.051	1.88	17.6	9.9	0.68	–	0.009	0.038	0.012	0.33 Ti
347	2.0[(1)]	0.060	1.88	17.44	9.85	0.77	–	0.073	0.038	0.011	0.79 Nb

[a] FN measured on weld using Ferritescope.
Solidification modes: [(1)] Austenitic-ferritic (AF), [(2)] Ferritic-austenitic (FA), the rest are fully austenitic (A).
[b] Accuracy of analysis 10 ppm.

luated for solidification cracking as well as HAZ crakking. The D9 alloys differed among themselves only in the level of titanium. The 316L and 316L(N) were used to study the effect of nitrogen addition, by controlled additions through the shielding gas during Varestraint testing. Nitrogen was varied in the range 0.04-0.19 %. Varestraint test specimens were prepared from the solution annealed blanks of 3 mm nominal thickness. Chemical analysis of weld metal composition for all elements, except nitrogen, was done by standard wet chemical techniques on chips extracted from the weld metal. Nitrogen analysis was obtained using a Leco nitrogen analyser using chips extracted from the weld metal.

Inconel 718 (IN-718) is required to be welded during manufacture of steam generator support structures of PFBR. This material exhibits slightly higher tendency to hot cracking than Inconel 600 or ENiCrFe-3 type materials, but is much more weldable than other precipitation-hardened nickel-base alloys. During initial fabrication trials, cracking was observed in cruciform joints made for qualification purposes. Investigations were therefore carried out [15, 16] using Varestraint test on weldability of IN-718 as well as ENiCrFe-3 weld metal for choice ofwelding consumable. Weldability testing in various joint configurations was then carried out using ENiCrFe-3 consumable [17]. The composition of IN-718 and ENiCrFe-3 consumable are shown in Table 2.

3.2 Hot cracking susceptibility testing

The specimens were prepared from sheet and tested using longitudinal Varestraint and Transvarestraint tests. In the longitudinal Varestraint test (LVT), specimens of dimensions 127 × 25 × 3 mm^3 were used and autogenous gas tungsten arc (GTA) weld beads were deposited along the length as shown in Figure 1. When the weld puddle reached the middle of the specimen, strain was applied pneumatically by bending rapidly over a ram of fixed radius. The straining was completed within 15 ms, so that the weld puddle was essentially *frozen* in position. The strain experienced by the specimen is related to the radius of the die block by the relation $e \cong t / 2r$,

where

e is the strain in the outer fibre,

t is the specimen thickness, and

r is the radius of the die block.

In the Transvarestraint test (TVT), the weld bead was applied transverse to the specimen length (Figure 1). Run-on and run-off tabs were attached by tack welding on the underside so that the weld bead was long enough to ensure thermal equilibrium at the instant of straining. Welding conditions used for testing were current 100 A at 12 V, welding speed 4.2 mm.s^{-1}, and shielding gas flow rate of 12 l.min^{-1}.

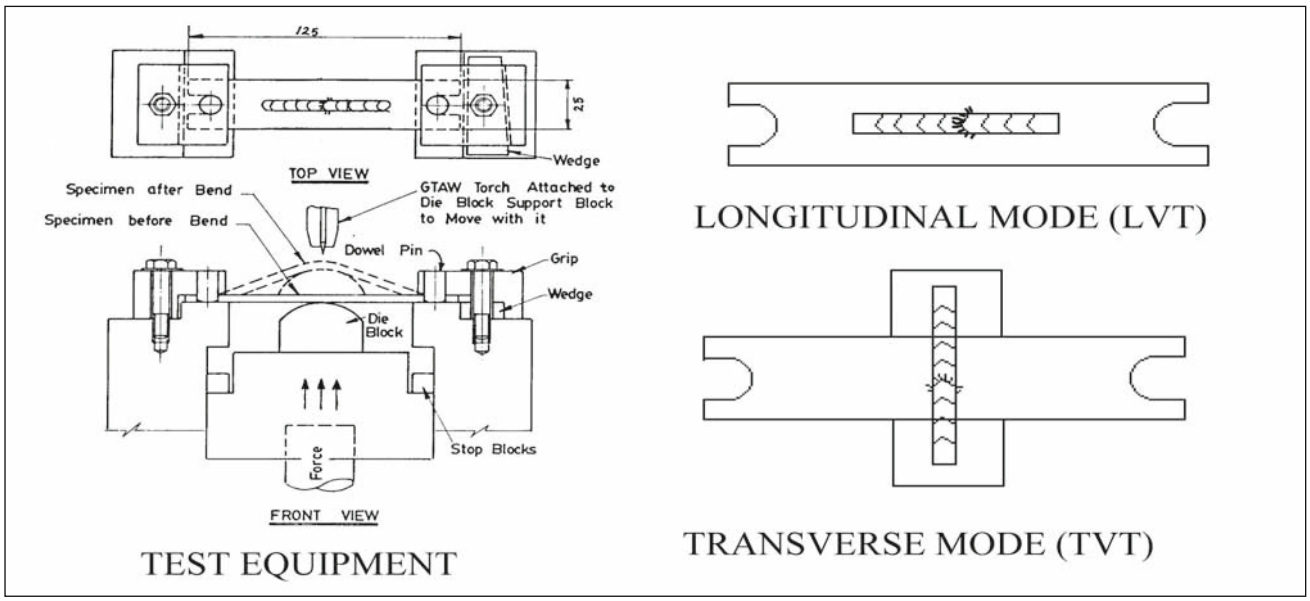

Figure 1 – Schematic diagram of moving torch TIG-A-MA-JIG Varestraint testing set-up, showing equipment, test procedure, and weld orientation in longitudinal and Transvarestraint mode

Table 2 – Chemical compositions (in wt-%) of the nickel-base alloy weld metals tested

Material	Ni	Cr	Fe	Mo	Nb	Al	Ti	Mn	Si	C	S	P
IN-718 A	52.9	18	18.8	3.0	5.03	0.21	0.93	0.06	0.05	0.06	0.001	0.003
IN-718 B	53.1	18.3	19.7	2.97	4.97	0.6	0.96	0.13	0.1	0.075	0.001	0.005
ENiCrFe-3	65.9	19.7	4.44	1.37	2.23	–	0.078	5.48	0.56	0.05	0.007	0.012

In addition to fusion zone cracking, base metal HAZ (BMHAZ) and weld metal HAZ (WMHAZ) cracking were also studied using a three-bead test technique [14, 18]. In this technique, the test weld is applied to produce HAZ cracking by overlapping on a previously deposited weld bead on one side (WMHAZ) and in base metal on the other. Cracking in the base metal HAZ and weld metal HAZ occurring on either side of the test weld bead was then evaluated. To study the influence of nitrogen on cracking, nitrogen was added through the shielding gas. The cracking was evaluated using the conventional criteria of crack length. Light microscopy and EPMA/SEM-EDAX were used for identifying elemental segregation. The brittleness temperature range (BTR) is the temperature envelope surrounding the weld puddle, in which the presence of liquid films renders the weld metal susceptible to cracking. The BTR was derived from the maximum crack length by converting distance or time into temperature using the weld-cooling curve, which was measured using a W-5 %Re/W-26 %Re thermocouple. Electrochemical dissolution of austenite was used to extract secondary phase particles in the weld metal, which were then identified using X-ray diffraction analysis.

3.3 Criteria for evaluation of hot cracking susceptibility

The longitudinal and transverse Varestraint test results for the ten austenitic stainless steels, comprising 316L SS, 316L(N) SS, 347 SS, 321 SS, three heats of Alloy D9 and three heats of 304L SS, were studied in order to compare cracking assessments by these two tests. The evaluation criteria for fusion zone cracking were critically examined. It was found that the total crack length criterion (TCL) derived from the longitudinal Varestraint test may not reflect true material behaviour under conditions of varying bead geometry and welding parameters. On the other hand, BTR derived from the transverse Varestraint test was a more consistent and accurate determinant of material behaviour. It was shown that BTR can be derived from the longitudinal Varestraint test also, through the use of a maximum crack distance (MCD) parameter [19] (Figures 2 and 3). Another advantage of the longitudinal test is that it

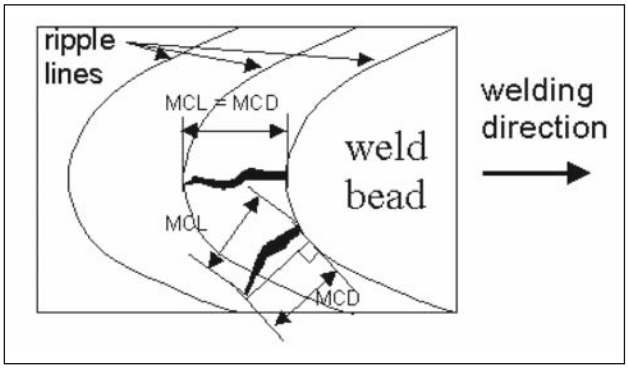

Figure 2 – The concept of maximum crack distance (MCD) in relation to maximum crack length (MCL) in longitudinal Varestraint test

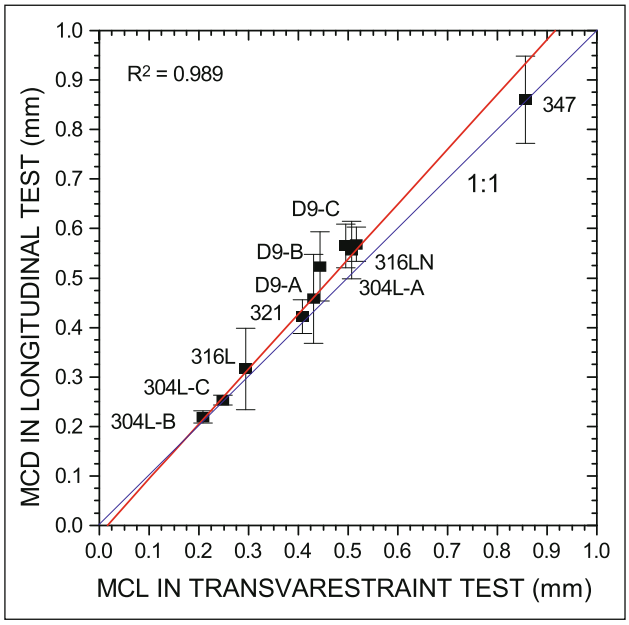

Figure 3 – Correlation between MCL in transverse Varestraint and MCD in longitudinal Varestraint tests

enables simultaneous assessment of fusion zone and HAZ cracking in the same sample [18]. Further, a new relation has been proposed between total crack length and BTR considering the area density of cracking [20] (Figure 4). This relation enables comparison across the large amount of data available worldwide using these two tests.

4 HOT CRACKING SUSCEPTIBILITY OF SOME AUSTENITIC STAINLESS STEELS

The effects of titanium on cracking in Alloy D9 were investigated by testing three heats with titanium levels of 0.21, 0.32 and 0.42 wt-% titanium (designated D9-A, D9-B and D9-C respectively) apart from types 321 SS

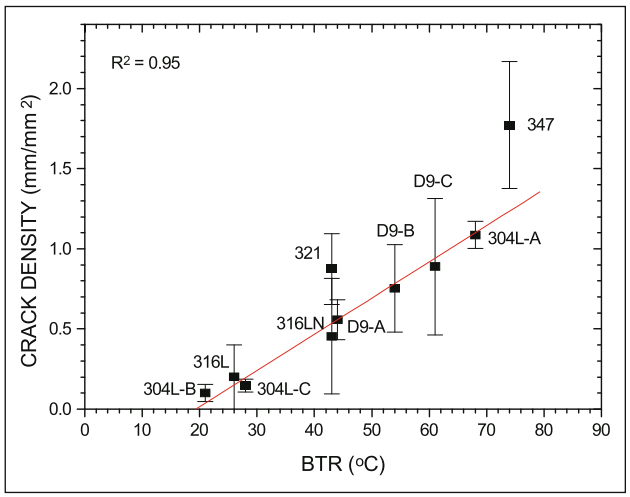

Figure 4 – Relation between BTR and crack density in longitudinal Varestraint test, crack density = TCL/(MCD×W) where W is the weld width

and 347 SS. The results showed that in the fusion zone, the cracking susceptibility of Alloy D9 was intermediate between that of primary ferritic-austenitic 321 SS and primary austenitic-ferritic niobium-stabilized 347 SS. Within the Alloy D9 heats, BTR increased by 20 % from 51 K in D9-A to 61 K in D9-C (Figure 5) as the titanium content increased. The 321 SS had the least susceptibility to cracking with BTR of 44 K because of a ferritic-austenitic mode of solidification (4.4 FN residual ferrite), while the 347 SS had a high cracking tendency owing to an austenitic-ferritic solidification mode and the formation of niobium-rich eutectics. EPMA analysis of hot cracks in Alloy D9 revealed segregation of titanium, carbon, nitrogen and sulphur to crack-faces and to segregate phases present inter-dendritically. A photomicrograph of hot cracks and segregation in D9-B weld metal is shown in Figure 6. Electrochemical extraction followed by X-ray diffraction analysis revealed that the segregate phases present in Alloy D9 and 321 SS were TiC, $TiC_{0.3}N_{0.7}$, and carbosulphides Ti_2CS and $Ti_4C_2S_2$ which apparently form eutectics with austenite and promote cracking. The relative amount of these phases increased with increasing titanium content, which was particularly high above a Ti/(C+0.857N) ratio of 3

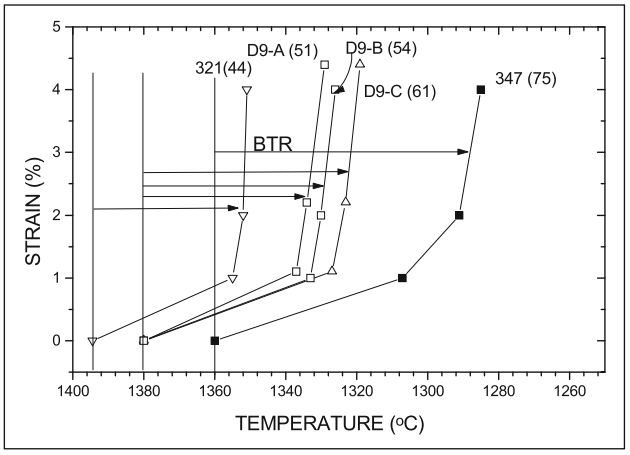

Figure 5 – Temperature-strain envelope for weld metal cracking in stabilized austenitic stainless steels, showing BTR

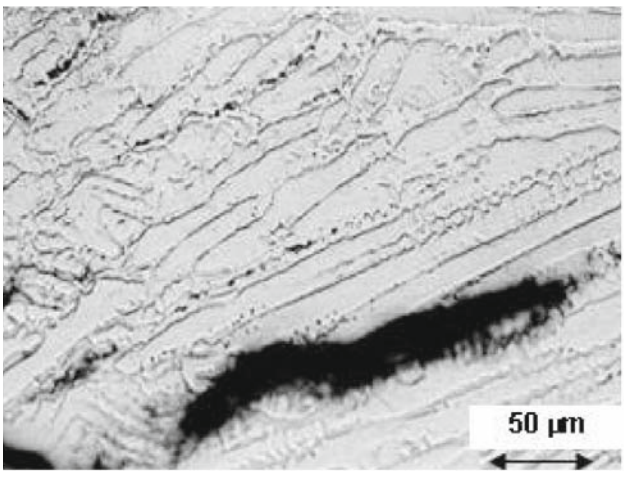

Figure 6 – Microstructure of D9-B weld metal showing cracking and segregates along inter-dendritic regions and crack extensions

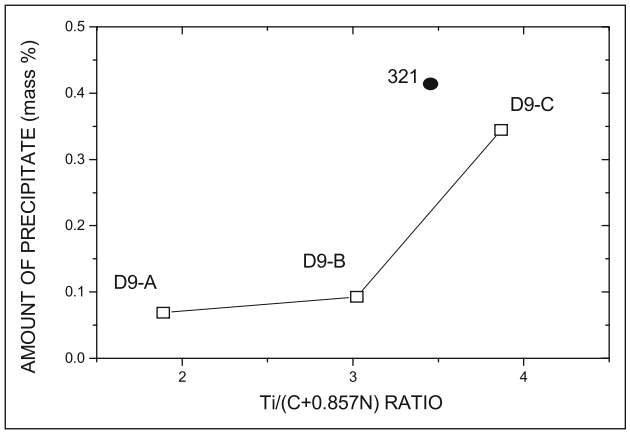

Figure 7 – Fraction of precipitate extracted as a function of Ti/(C+0.857N) in Alloy D9 and 321 SS

(Figure 7). The factor 0.857 represents the ratio of the mass numbers of carbon and nitrogen.

Brittleness temperature range (BTR) measurements were derived from maximum crack length values obtained in the Varestraint test. The variation of BTR as a function of strain for D9 and 316L(N) stainless steel base metals, and the modified 316 weld metals are shown in Figures 8 a) and 8 b), respectively [21–23]. It is well known that BTR and solidification cracking are a strong function of the solidification mode in stainless steels. Therefore, the cracking data is shown as a func-

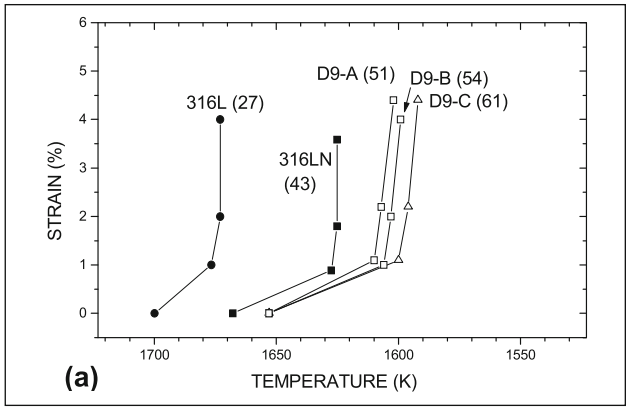

a) D9 and 316L(N) base metals

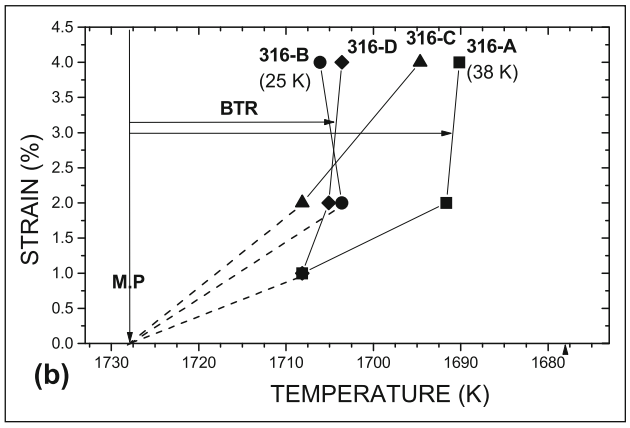

BTR values are given in parentheses

b) modified 316 weld metals (0.07-0.12 wt-%N)

Figure 8 – Brittleness temperature range (BTR) of austenitic stainless steels

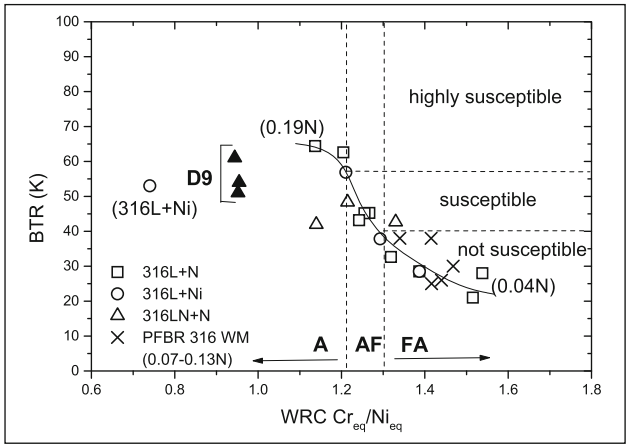

Experimentally observed solidification mode boundaries are indicated
(A: austenitic, AF: austenitic/ferritic, and FA: ferritic/austenitic).

Figure 9 – Solidification cracking in D9, 316LN and modified 316 weld metals as a function of WRC Cr_{eq}/Ni_{eq} ratio

tion of WRC Cr_{eq}/Ni_{eq} (chromium equivalent to nickel equivalent) ratio in Figure 9.

In Figure 9, data for D9, 316L(N) and modified 316 weld metals are shown. Also represented are data corresponding to nitrogen-added 316L or 316L(N) base materials in the range 0.04–0.19 %N. A few data are also shown for nickel-added compositions for comparison. The BTR values are low for high Cr_{eq}/Ni_{eq}, i.e., above a value of 1.3, which corresponds to a ferritic solidification mode. Stainless steel base and weld metals solidifying in the FA mode of solidification have BTR of 30 K or lower and are highly resistant to solidification cracking. The cracking tendency increases with decreasing Cr_{eq}/Ni_{eq} ratio, i.e., decreasing ferrite content, while the solidification mode changes to AF (austenitic/ferritic) and to A (fully austenitic). The modified 316 weld metal is observed to be in the safe regime with FA solidification mode. However, the D9 alloys being fully austenitic can be considered to be highly susceptible to solidification cracking [24].

However, solidification cracking is also a function of the level of impurity elements sulphur, phosphorus and minor elements such as titanium and silicon. Although a direct correlation between the composition, impurity levels and cracking is not available at present, the diagram of Kujanpaa *et al*. [25] of Cr_{eq}/Ni_{eq} vs. phosphorus + sulphur (P+S) content can be used, with the Cr_{eq} and Ni_{eq} corresponding to that of Hammar-Svensson (H-S). In this diagram (Figure 10), susceptible compositions lie in the region of $Cr_{eq}/Ni_{eq} < 1.5$ and P+S > 0.015 wt-%. Much higher impurity levels could be tolerated for higher Cr_{eq}/Ni_{eq} ratios and such compositions were not susceptible to cracking. In Figure 10, cracking data for D9 and 316LN stainless steels have been shown in terms of Hammar-Svensson (H-S) Cr_{eq}/Ni_{eq} ratio and P+S contents. The BTR values at 4 % strain corresponding to each material are indicated within parentheses beside each datum point. The important feature in Figure 10 is that unstabilised stainless steels fit reasonably well into the diagram, with low-BTR compositions finding a place in the less susceptible regions and the high-BTR 304L-A and D9 alloys are placed in the *highly susceptible* portion. On the other hand, the stabilized stainless steels 321 and 347 show much higher susceptibility for equivalent Cr_{eq}/Ni_{eq} ratio and impurity content, compared to the unstabilised varieties. This is presumably because of the potent influence of titanium and niobium on the cracking tendency that is not taken into account in this diagram. The D9 alloys, despite having low P+S (0.014 wt-%), show high susceptibility, which can be attributed to the presence of titanium.

4.1 Effect of nitrogen on hot cracking in 316L stainless steel

The effect of nitrogen in two alloys 316L SS and 316L(N) SS were investigated by conducting hot crakking tests with nitrogen addition through the shielding gas. Six nitrogen levels in the range 0.036–0.187 wt-% were tested for 316L SS and three nitrogen levels in the range 0.073–0.189 wt-% in 316L(N) SS. The nitrogen analysis and the ferrite content of the weld metals are shown in Table 3.

Nitrogen addition produced significant coarsening of the primary solidification structure, as shown in Figure 11, which shows the weld metal microstructures in 316L and 316L(N) at various N levels. The primary dendrite arm spacing (λ_1) could be related to the nitrogen content by a relation of the form $\lambda_1 = A(C)^{0.5}$ (Figure 12),

where

C is the nitrogen content, and

A is a factor including thermal variables and partition coefficient for nitrogen, which are assumed to remain constant.

It must be noted that all the nitrogen-added weld metals solidify in the austenitic mode. In the weld metal, nitrogen increased cracking in the higher-impurity content 316L (0.047 wt-% P+S), while there was no significant effect on cracking in the 316L(N) (0.032 wt-% P+S).

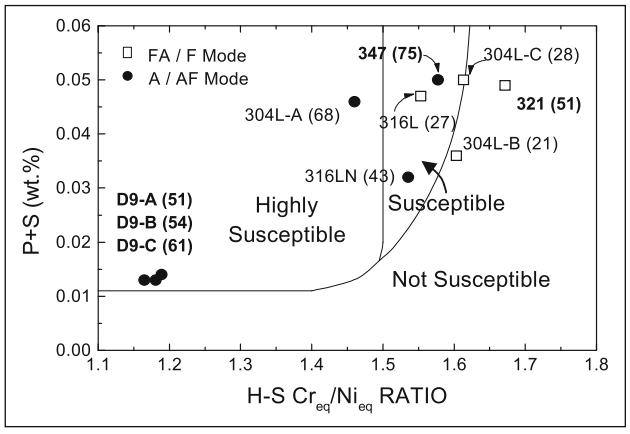

Figure 10 – Modified Suutala diagram showing hot cracking behaviour as a function of Hammar-Svensson Cr_{eq}/Ni_{eq} and P+S content

Table 3 – Nitrogen contents in shielding gas and weld metal with corresponding ferrite contents and solidification modes

Material	Nitrogen content in		Ferrite No. (FN)	Solidification mode
	Shielding gas (vol.-%)	Weld metal (wt-%)		
316L(N)	0	0.073	0.7	AF
	2.0	0.139	Nil	A
	5.0	0.189	Nil	A
316L	0	0.036	2.7	FA/AF
	0.4	0.0715	1.7	AF
	0.5	0.101	0.2	AF
	1.0	0.108	Nil	A
	2.0	0.116	Nil	A
	3.0	0.14	Nil	A
	5.0	0.187	Nil	A

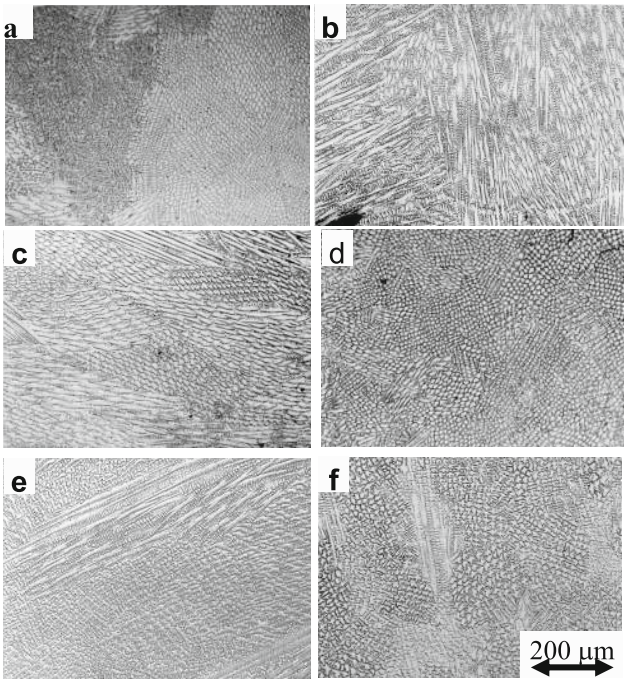

Microstructure in (a) is FA/AF, while rest are fully austenitic.

Figure 11 – Solidification structure of 316L/316L(N) weld metals: a) 316L (0.04 %N); b) 316L (0.12 %N); c) 316L (0.19 %N); d) 316L(N) (0.073 %N); e) 316L(N) (0.12 %N); and f) 316L(N) (0.19 %N)

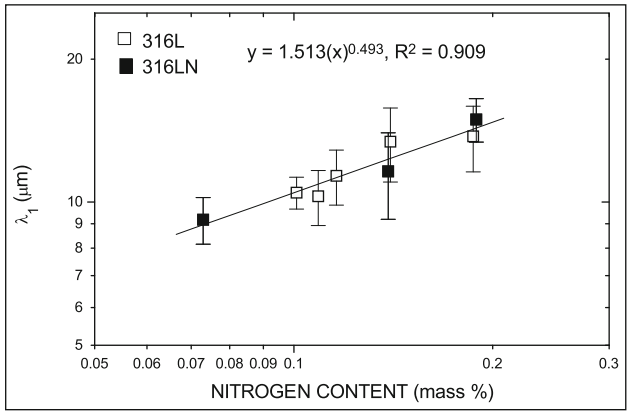

Figure 12 – Primary dendrite arm spacing of 316L and 316L(N) weld metals as function of nitrogen content

The dependence of the effect of nitrogen on the levels of impurity elements present was further established by tests in which nickel addition was used to produce an austenitic microstructure. The relation between composition and cracking is presented in Figures 13 a) and 13 b), where BTR is shown as a function of nitrogen level and WRC Cr_{eq}/Ni_{eq} ratio, respectively.

In 316L, both nickel and nitrogen additions produced an increase in cracking that was attributable to a change in solidification mode from ferritic to austenitic. However, nitrogen addition appeared to increase cracking to a level greater than that with nickel. Nitrogen is not known to form low-melting eutectics during solidification with any of the constituents of stainless

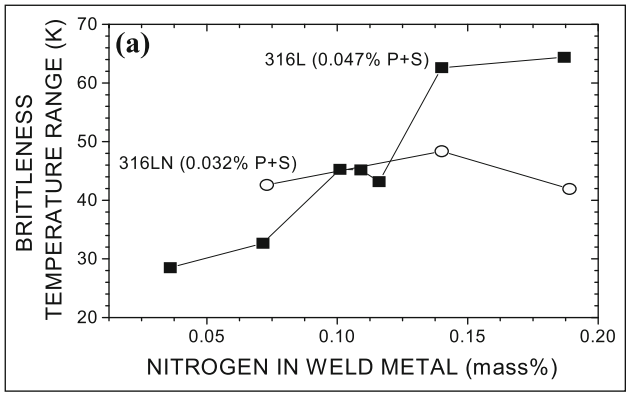

a) as a function of nitrogen content

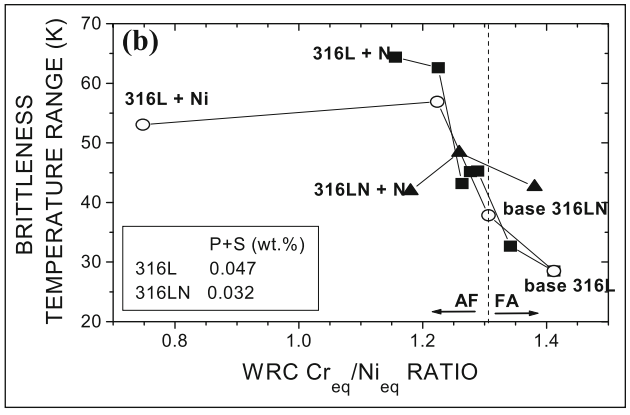

b) as a function of WRC Cr_{eq}/Ni_{eq}, including effect of nickel

Figure 13 – BTR of weld metals

steel, unlike carbon, which forms $M_{23}C_6$ eutectics with austenite. Electrochemical extraction of weld metal also did not reveal any phase other than Fe_4N that is known to form in the solid state. While the exact mechanism by which nitrogen acts to exercise these effects is not known, it is believed that nitrogen increases cracking by influencing segregation of other elements including impurities such as phosphorus and sulphur.

4.2 Effect of titanium and nitrogen on hot cracking

Specifically, the effect of titanium and nitrogen on crakking in D9 and 316LN is of interest for PFBR fabrication. Extensive studies have been carried out on fusion zone and HAZ cracking in these materials [22]. Investigations of cracking in D9 welds showed that the cracking is due to segregation of titanium, sulphur, nitrogen and carbon to the grain boundaries. The weld metal tends to absorb a high level of nitrogen (about 200 ppm) during welding even with high purity gas, over and above the nitrogen level present in the base material. Since nitrogen participates in cracking, it is relevant to represent the effect of titanium in terms of Ti/(C+0.857N) ratio (a factor of 0.857 is used for N to account for the difference in atomic weight between C and N), as shown in Figure 14. It is observed from Figure 14 that while titanium does not have a great influence on fusion zone cracking, the increase in HAZ cracking with Ti/(C+N) is significant.

The nitrogen effect on cracking in 316LN base metal [23] as well as modified 316 base metals [24] is well represented in Figure 9. In Figure 9, data for two types of weld are shown; nitrogen-added 316 and 316L(N) with 0.04–0.19 %N, and modified 316 weld metals with 0.07–0.12 %N while maintaining Cr_{eq}/Ni_{eq}. The essential observations from these data are that nitrogen has no detrimental effect on cracking if Cr_{eq}/Ni_{eq} is maintained to obtain a favourable solidification mode in the weld metal. Nitrogen could be detrimental if ferrite is absent or solidification mode becomes austenitic (A mode) and when sulphur level is greater than 0.01 %. This situation is possible during autogenous welding of base metal or when HAZ cracking is envisaged. During structural welding of components for PFBR the risk of cracking during autogenous welding is small due to stringent specifications, particularly for impurity elements. HAZ cracking has been shown to be a strong function of ferrite content or ferrite potential of the underlying material, but is likely only in extremely high restraint situations. Both these factors are not a serious concern during structural welding for PFBR.

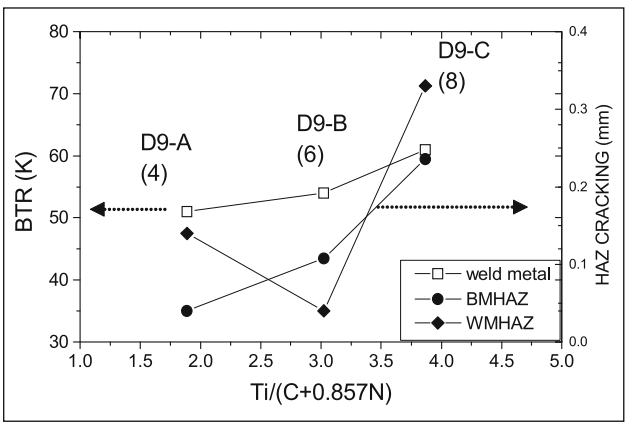

Figure 14 – Effect of Ti/(C+N) ratio on cracking in D9 weld metal, base metal and weld metal HAZ (nominal Ti/C ratio in parentheses; HAZ cracking: right-hand side y-axis)

4.3 Effect of composition on hot cracking in the HAZ

The HAZ cracking behaviour of ten austenitic stainless steels was studied using three-bead test technique both in base metal and weld metal HAZ. Cracking was evaluated using a maximum crack length criterion, which could be related to the BTR for HAZ cracking [27]. The maximum crack lengths in the base and weld metal HAZ for the *stabilized austenitic stainless steels* are shown in Figures 15 a) and 15 b), respectively. Among the D9 alloys, cracking increased strongly as a function of Ti/(C+0.857N), with an effect much greater than in the fusion zone. Among the commercial heats of 347 SS and 321 SS, the cracking increased with decreasing ferrite potential. Generally, cracking in the WMHAZ was greater than that in the BMHAZ. Although

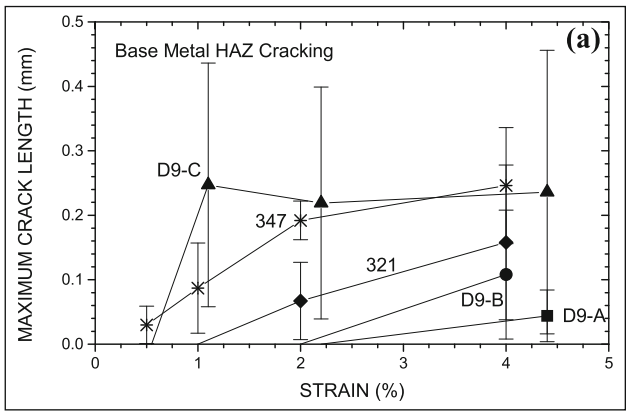

a) Base metal HAZ cracking

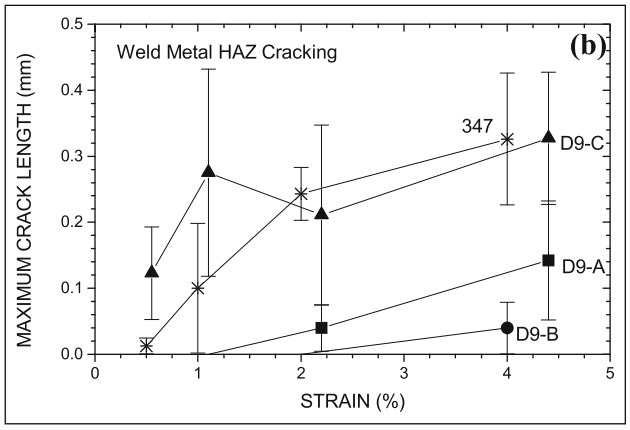

b) Weld metal HAZ cracking

Figure 15 – HAZ cracking behaviour of stabilized austenitic stainless steels Alloy D9, 321 SS and 347 SS

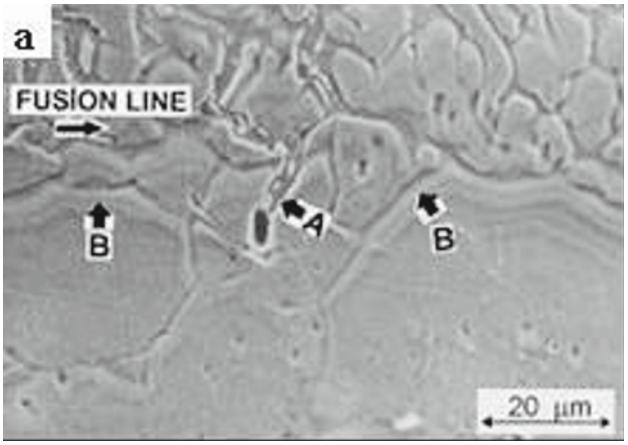

a) SEM micrograph of cracking in BMHAZ showing grain boundary migration and backfilling

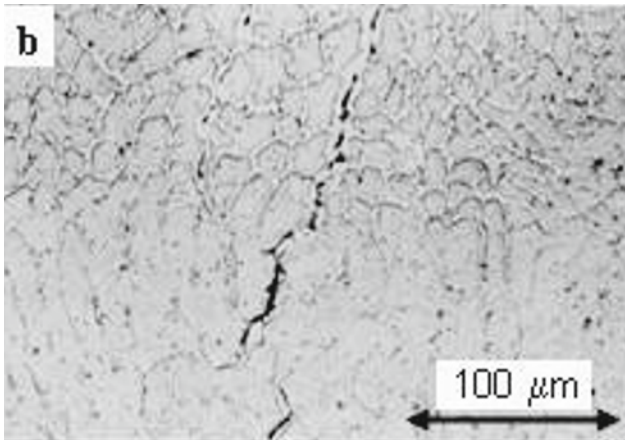

b) Optical micrograph of WMHAZ cracking showing continuity of liquid film containing segregates across fusion line

Figure 16 – HAZ cracking in D9-B

the titanium-bearing 321 SS showed high cracking in the BMHAZ, the ferrite present in the underlying weld bead was effective in completely preventing cracking in the WMHAZ.

In Alloy D9, the cracking was associated with several interesting microstructural features such as grain boundary migration, *ghost boundaries* and backfilling of cracks, as shown in Figures 16 a) and 16 b). Figure 16 a) is a SEM micrograph of BMHAZ cracking in D9-B, which shows liquated grain boundaries that have migrated, leaving behind traces of segregation that appear as *ghost boundaries* (marked B). The backfilled portions marked A in the figure exhibiting residual segregates are clearly connected to the fusion zone. This penetration of the liquid from the fusion zone into HAZ cracks is also visible in Figure 15 b), which shows WMHAZ cracking in the same material.

Base and weld metal HAZ cracking in *unstabilised austenitic stainless steels* are shown in Figures 17 a) and 17 b), respectively. In the BMHAZ, cracking was greater in the primary austenitic 316L(N) and 304L-A materials and was a function of the ferrite potential. Optical micrographs of BMHAZ cracking in 316L and 316L(N) are shown in Figures 18 a) and 18 b), respectively, where the considerable difference in grain size between the two HAZs is evident. Further, the liquation and grain boundary melting in the 316L(N) SS are much greater than in 316L SS. The lower ferrite potential could also explain the high degree of cracking of the 316L(N) SS in the weld metal HAZ [Figure 17 b)]. Previous studies have shown the beneficial effect of a high ferrite potential in reducing HAZ cracking [26].

4.4 Effect of nitrogen on hot cracking in HAZ of 316L stainless steel

Weld metal HAZ cracking was studied as a function of nitrogen content in 316L and 316L(N), as in the case of fusion zone cracking. The maximum crack length in the WMHAZ is shown as a function of nitrogen content in Figure 19, where it is observed that cracking increases with nitrogen content for both 316L and 316L(N) SS. However, in the fully austenitic regime, the cracking shows saturation. Typical micrographs of WMHAZ crakking in the 316L and 316L(N) SS with 0.19 wt-%N level are shown in Figures 20 a) and 20 b), respectively. In 316L SS, cracking was characterised by the presence of smooth grain boundaries that are easily wetted. On

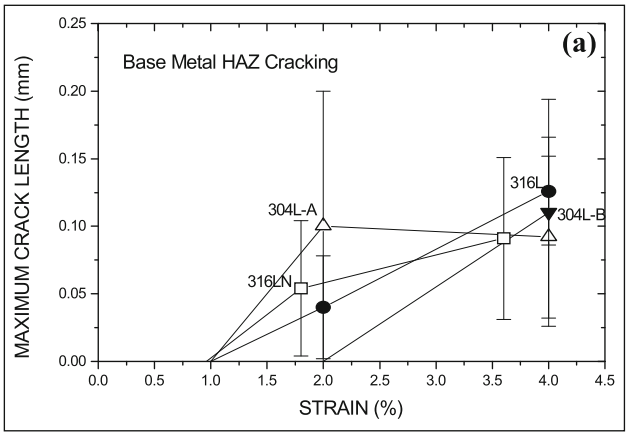

a) in base metal

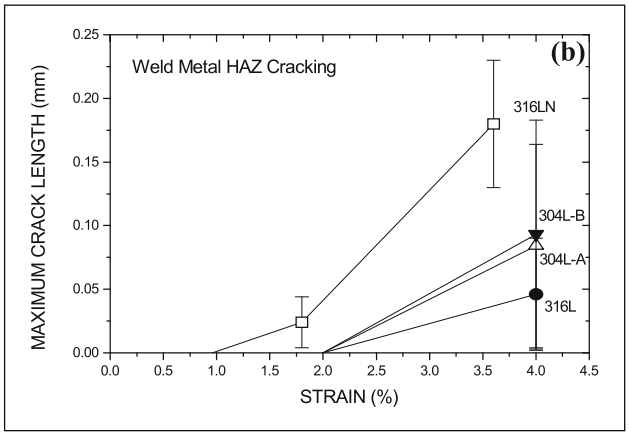

b) in weld metal

Figure 17 – HAZ cracking in unstabilised austenitic 316L, 316L(N) and 304L SS

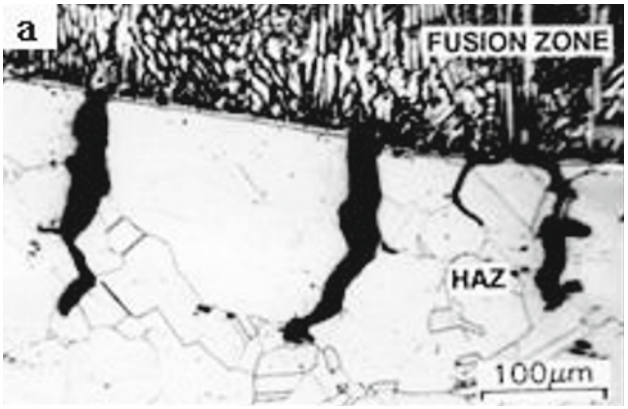

a) 316L showing large HAZ grain size

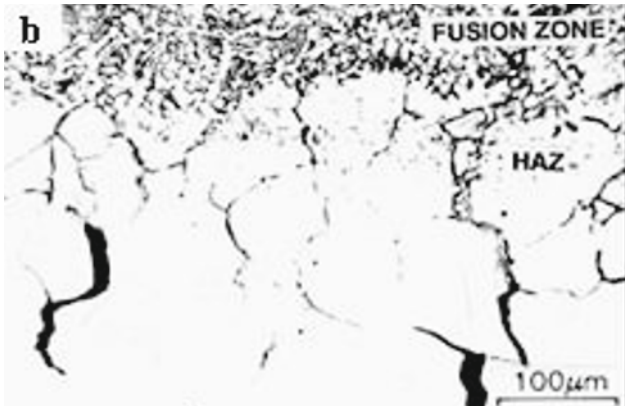

b) 316L(N) showing wide partially melted zone and liquation

Figure 18 – Microstructures of HAZ cracking in unstabilised austenitic SS

the other hand, the crack paths were more convoluted in the 316L(N), as shown in Figure 20 b). The lower cracking tendency of the 316L(N) SS with increasing nitrogen content is probably due to the lower S level in this material. This is consistent with the recent work [28], which has shown that sulphur is more significant than phosphorus in determining HAZ cracking.

4.5 Correlation between composition and hot cracking in the fusion zone

A correlation was attempted between composition and hot cracking in austenitic stainless steels. The composition was represented in terms of WRC Cr_{eq}/Ni_{eq} ratio and P+S content, and hot cracking in terms of BTR. Correlation was also attempted using the Hammar-Svensson (H-S) equivalent formulae [25]. The WRC Cr_{eq}/Ni_{eq} ratio was found superior to other equivalent formulae in relation to cracking. The BTR criterion enabled much better correlation with cracking than total crack length in the fusion zone.

4.6 Hot cracking susceptibility assessment criteria

In actual welds, the amount of strain experienced by the weld metal is difficult to estimate in view of complex geometric and thermal conditions. Hence a controlled strain applied on a geometrically simple specimen is preferred for evaluation of cracking tendency. Several tests exist that satisfy the above condition, such as the Varestraint test, the PVR test (programmierter Verformungsrisstest) and the Sigmajig test. These tests use any of several criteria such as total crack length, maximum crack length, strain threshold, strain rate threshold and brittle temperature range. While these criteria are very useful for comparison, direct application of hot cracking test data to actual fabrication is possible only if the restraint in the latter case can be quantified.

Application of Varestraint test criteria such as crack lengths and BTR to practical welding situations is complicated by the fact that in the actual case, strain, strain rate and stress are difficult to quantify as a function

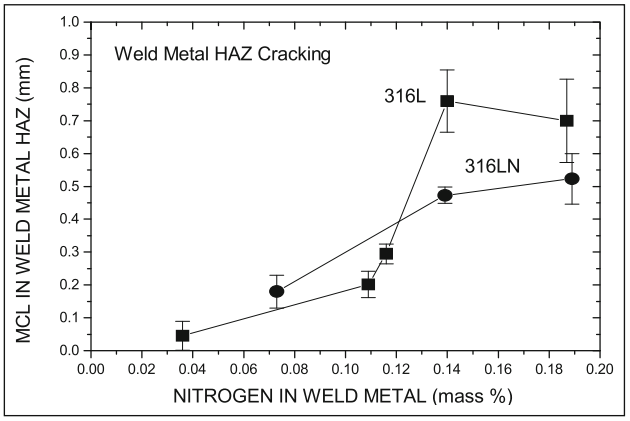

Figure 19 – WMHAZ cracking in 316L and 316L(N) SS as a function of nitrogen content

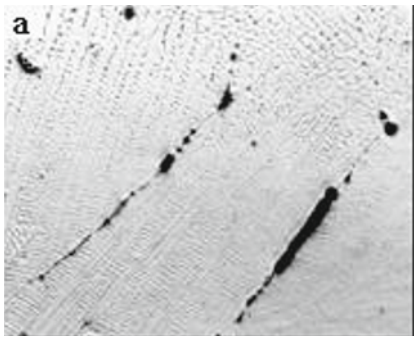

a) in 316L SS

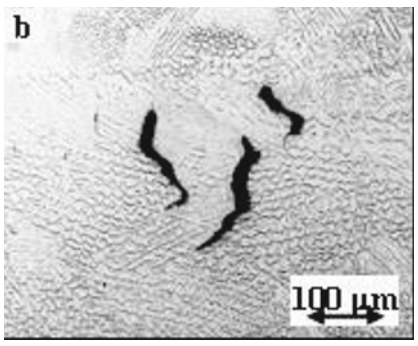

b) in 316L(N) SS

Figure 20 – Microstructures of WMHAZ cracking at 0.19 %N

of weld geometry. Tests such as Y-groove test [29] or circular patch test [4] or actual weld joints have been used for correlation with Varestraint test results. However, there are reports that ranking based on BTR is more reliable than TCL from the Varestraint test. A review of the literature thus shows that there is no universal choice of criteria for cracking assessment when applied to actual welding situations. Investigations by the authors show that the TCL parameter is subject to variations because of weld bead geometry, while BTR is not influenced by these factors that are related to fluid flow effects in the weld pool. It has been shown [21] (Figure 21) that if TCL is normalised using the weld width, the correlation with BTR is very good. It must be mentioned that BTR parameter has been widely used in Japan for the past three decades [30].

It is observed from Figure 3 that the modified 316 weld metal for PFBR with limits of ferrite content of 3–7 FN is located in the FA mode of solidification and would essentially be free from hot cracking in the weld metal and HAZ. However, problems could arise during welding of D9 for wrapper and clad tubes and welding conditions may require careful optimisation.

5 HOT CRACKING SUSCEPTIBILITY OF INCONEL 718

The effect of heat input on solidification cracking [15], expressed as maximum crack length (MCL) of Inconel 718 is shown in Figure 22, where it is observed that cracking increases with increasing heat input, i.e. decreasing cooling rate. This is in contrast to the cracking in stainless steel weld metal where hot cracking is not sensitive to heat input in the normal range of welding. The distinctive behaviour of Inconel 718 weld metal is due to the influence of heat input on niobium segregation, which is responsible for the cracking. The relative cracking tendencies of Inconel 718 and ENiCrFe-3 weld metals are shown [16] in Figure 23, where it is observed that the latter is much less prone to cracking. ENiCr-Fe-3 consumable was therefore chosen for welding Inconel 718 for steam generator. Apart from solidification cracking, Inconel 718 is also susceptible to HAZ cracking, which can be minimised by welding in the low temperature 1 198 K (925 °C) /1 h solutionised condition.

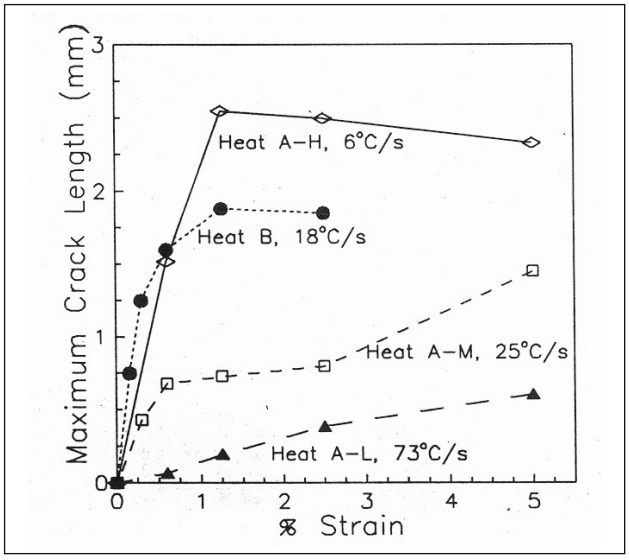

Cooling rate $t_{8/5}$ is indicated for each curve.

Figure 22 – Effect of heat input on solidification cracking of Inconel 718

Weldability of Inconel 718 using E NiCrFe-3 consumable was examined [17] in several joint configurations such as (a) 4 mm to 4 / 2 mm T, (b) 10 mm rod to 4 mm strip, (c) 20 mm diameter ferritic steel rod to 4 mm strip and (d) 4 mm strip butt joint configurations as part of procedure qualification. The welds were subjected to LPT, radiography and mechanical testing depending upon the joint configuration.

Of the configurations welded, butt joints showed the least incidence of defects, although lack of fusion was present occasionally due to poor fluidity of weld metal. Pulsed welding is suggested to improve fusion

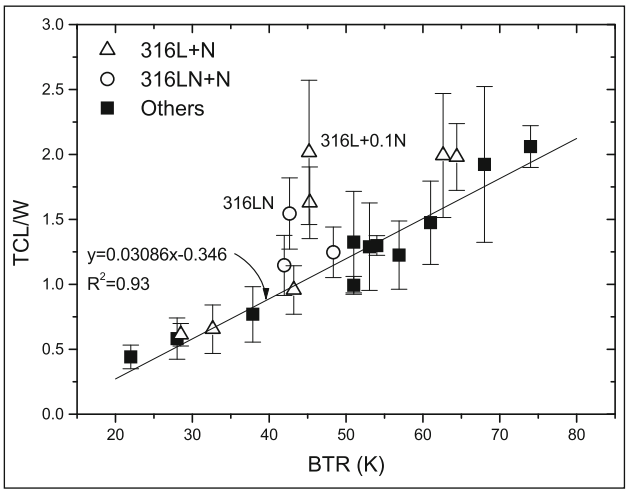

Figure 21 – Correlation between normalised total crack length (TCL/W, W-weld width) and brittleness temperature range (BTR) criteria

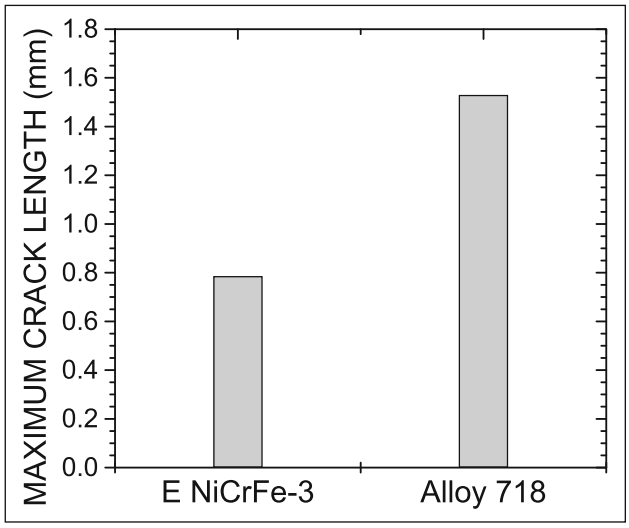

Figure 23 – Relative solidification cracking tendencies of ENiCrFe-3 and Inconel 718 weld metals at 4 % strain

by increasing welding current without increasing heat input. Tensile strength and ductility of the butt welds made using ENiCrFe-3 filler were 50–60 % of that of the base metal in the aged condition. Solution annealing at 1 338 K (1 065 °C) is generally recommended in the literature to improve tensile and bend ductility. Although the joints for steam generator tube support structures are not highly stressed, the study indicates that proper joint preparation and use of techniques such as pulsed welding would be beneficial in obtaining sound joints.

6 CONCLUDING REMARKS

Weldability aspects of FBR materials during fabrication have been discussed. The importance of hot cracking evaluations in determining the fabrication weldability of austenitic stainless steels has been illustrated. Finally, it has been shown how the life of dissimilar metal joints for steam generators can be extended by suitable choice of joint configuration and welding consumables.

The weldability investigations on 316L(N) and D9 weld metals, and on Inconel 718 alloy have generated useful data on several aspects of fabrication using these materials. The following are the conclusions and recommendations for welding these materials.

1. Weldability of austenitic stainless steels as measured using brittleness temperature range criterion (BTR) from the Varestraint test correlated well with the experimentally observed solidification mode and according to the WRC-92 equivalent formulae. Normalising total crack length (TCL) with weld width gave better correlation with BTR, while variability was high when TCL alone was used.

2. Nitrogen in modified 316 weld metal within the specified range of 0.06-0.1 % and up to 0.12 % was not detrimental to weldability. Nitrogen in fully austenitic weld metal resulted in increased weld metal and HAZ cracking when sulphur level was over 0.01 %.

3. Alloy D9 exhibited sensitivity to solidification and HAZ cracking because of the fully austenitic microstructure and due to the presence of titanium, sulphur, carbon and nitrogen in the weld metal. Cracking, particularly in the HAZ, increased with Ti/(C+N) ratio. From the point of view of weldability, it is desirable to maintain this ratio as low as possible.

4. For welding clad and wrapper tubes of Alloy D9 for PFBR, single-pass welding is preferable in view of its propensity to HAZ cracking. Use of pulsed GTA or micro-plasma process is recommended for clad and wrapper tubes. No special precautions are considered necessary for 316L(N).

5. Weldability studies on Inconel 718 using Varestraint test showed that cracking in the weld metal increased with heat input. ENiCrFe-3 type of filler material was preferable over matching consumable to weld Inconel 718 as its cracking tendency was much lower. Welding of various joint configurations of Inconel 718 using this filler showed that satisfactory welding requires (a) good joint preparation and (b) pulsed welding, to improve weld bead penetration and prevent lack of fusion, and (c) post-weld heat treatment to restore mechanical properties, if desired.

REFERENCES

[1] Dixon B.F., Welding Journal, 1989, 68, 171s.

[2] ASME Boiler and Presser Vessel Code, Code case N-47, 1989.

[3] Marshall P.: Austenitic stainless steels: Microstructure and mechanical properties, Elsevier Applied Science Publishers, London, 1984, 283.

[4] Lundin C.D., Lee C.H., Qiao C.Y.P.: Group sponsored study – Weldability and hot ductility behaviour of nuclear grade austenitic stainless steels, Final Report, University of Tennessee, Knoxville, USA, 1988.

[5] Brooks J.A., Thompson A.W., International Materials Reviews, 1991, 36, 16.

[6] Robinson J.L., Scott M.H., Philosophical Transactions of the Royal Society of London, 1980, 295A, 105.

[7] Masumoto I., Takami K., Kutsuna M., Journal of the Japanese Welding Society, 1972, 41, 1306.

[8] Rodriguez P., Mannan S.L., Indian Journal of Technology, 1990, 28, 281.

[9] Tamura H., Watanabe T., Transactions of the Japanese Welding Society, 1973, 4, 30.

[10] Brooks J.A., Welding Journal, 1974, 53, 517s.

[11] Zhitnikov N.P., Welding Production, 1981, 3, 14.

[12] Ogawa T., Tsunetomi E., Welding Journal, 1982, 61, 82s.

[13] Matsuda F., Nakagawa H., Katayama S., Arata Y., Transactions of the Japanese Welding Research Institute, 1983, 2, 89.

[14] Lundin C.D., Lingenfelter A., Grotke G., Lessman G., Mathews S., WRC Bulletin, 1982, 280.

[15] Shankar V., Muralidharan B.G., Srinivasan G., Gill T.P.S., Proceedings of International Welding Conference, Indian Institute of Welding, Mumbai, 1996, Paper A-056.

[16] Muralidharan B.G., Shankar V., Gill T.P.S., Proceedings of National Welding Seminar, Indian Institute of Welding, Bangalore, 1997, 329.

[17] Srinivasan G., Shankar V., Gill T.P.S., Sethi V.K., Proceedings of International Welding Conference, Indian Institute of Welding, New Delhi, 1999, 617.

[18] Lundin C.D., Menon R., Lee C.H., Osorio V.: Welding research: The state of the art, Proceedings of JDC University Research Symposium, ASM, 1986, 33.

[19] Lin W., Nelson T., Lippold J.C., Proceedings of 8th Annual North American Welding Research Conference, AWS, EWI and TWI, 1992, 1.

[20] Shankar V.: Role of compositional factors in hot crakking of austenitic stainless steel weldments, Ph.D. Thesis, Indian Institute of Technology, Madras, 2000.

[21] Shankar V., Gill T.P.S., Mannan S.L., Sundaresan S., Science and Technology of Welding and Joining, 2000, 5, 2, 91.

[22] Shankar V., Gill T.P.S., Terrance A.L.E., Mannan S.L., Sundaresan S., Metallurgical and Materials Transactions A, 2000, 31A, 3109.

[23] Shankar V., Gill T.P.S., Mannan S.L., Sundaresan S., Materials Science and Engineering, 2003, 343, 170.

[24] Shankar V., Gill T.P.S., Thamban M., Patel P., Proceedings of Symposium on Joining of Metals, Welding Research Institute, Tiruchirapalli, India, 2000, Paper WM-25.

[25] Kujanpaa V., Suutala N., Takalo T., Moisio T., Welding Research International, 1979, 9, 2, 55.

[26] Kujanpaa V.P., David S.A., White C.L., Welding Journal, 1986, 65, 203s.

[27] Lin W., Lippold J.C., Baeslack W.A., Welding Journal, 1993, 82, 135s.

[28] Li L., Messler R.W., Welding Journal, 1999, 88, 387s.

[29] Miura M., Journal of Sumitomo Metal, 1981, 34, 1, 201.

[30] Matsuda F., Advances in Welding Metallurgy, AWS, 1990, 19.